2003 4th IEEE Workshop on Signal Processing
Advances in Wireless Communications

JOINT TIME-DELAY AND FREQUENCY OFFSET SYNCHRONIZATION FOR CDMA ARRAY-RECEIVERS

Besma Smida, Sofiène Affes, and Paul Mermelstein

INRS-Télécommunications, Université du Québec
Place Bonaventure, 800, de la Gauchetière Ouest, Suite 6900
Montréal, Québec, H5A 1K6, Canada

ABSTRACT

This paper addresses the problem of joint time-delay and frequency synchronization in the CDMA receiver STAR. We observe that its space/time structural approach enables us to decouple time and frequency offsets. We thus introduce a new procedure based on space/time separation that implements a simple linear regression approach for both time-delay and frequency synchronization. We analyze the performance of this procedure in an unknown time-varying channel with multipath and carrier offset. Simulations show that the modified STAR provides significant performance gain over its previous version. The link-level gain is more than 3 dB for BPSK (128 kb/s) when the frequency offset equals 0.1 ppm (i.e., 200 Hz). This gain increases at higher frequency offsets and small-constellation modulations.

1. INTRODUCTION

In wireless communication systems, besides the effects of channel attenuation and multipaths, the transmitted signal will be received with a frequency offset due to the motion of the mobile and an inevitable carrier frequency difference between the transmitter and the receiver. Estimation of the frequency offset and the channel response is therefore essential for high-speed CDMA systems. In addition, time and frequency synchronization is very important for antenna-array receivers because an incorrect frequency offset and/or multipath timing will degrade performance and reduce spectral efficiency.

In previous work, we presented a CDMA array-receiver STAR, the spatio-temporal array receiver [1]. STAR performs very accurate and fast channel acquisition and timing and hence achieves high spectrum efficiencies at low complexity. So far, however, we investigated the time-delay synchronization [3] and carrier frequency offset recovery [2] separately. In this paper, we address the problem of rapid and accurate joint synchronization in time and frequency.

Work supported by Bell/Nortel/NSERC Industrial Research Chair in Personal Communications and by the NSERC Research Grants Program.

Although both the multipath channel and the carrier offset must be estimated, carrier synchronization and channel identification have traditionally been treated as separate problems. Most research in channel identification implicitly assumes that the carrier offset has been properly compensated. Similarly many existing carrier recovery techniques consider only flat channels.

Joint estimation of multipath and carrier offset was previously shown to be advantageous [4]. The optimum joint estimation of channel and frequency offset can be solved based on the maximum likelihood (ML) method. However, the ML solution requires extremely complex computations because of the multi-dimensional optimization [5]. References [6] and [7] proposed a subspace-based scheme for jointly estimating the channel response and the carrier offset, however this estimator still requires huge computational complexity.

We propose a joint time-delay and frequency synchronization procedure via space/time separation (see [1] for more details) in the context of the antenna-array receiver STAR. This new procedure implements simple Linear Regression (LR) for both frequency and time-delay synchronization. It is also a software-defined solution; the received signal is decorrelated, sampled and then processed using programmable digital signal processing. Numerical results show that the proposed algorithm compensates almost completely the performance loss due to high and low frequency offsets. The link-level gain is more than 3 dB for BPSK (128 kb/s) with frequency offset of 0.1 ppm. We also find that the performance gains increase at higher frequency offsets and small-constellation modulations.

2. SYSTEM MODEL

2.1. Data Model

We consider uplink transmission with M receiving antennas at the base station and consider a multipath Rayleigh fading channel with number of paths P and Doppler spread frequency f_D. We also assume a frequency offset Δf due to transmitter and receiver oscillator mismatch. The spread-

0-7803-7858-X/03/$17.00 ©2003 IEEE

ing factor, defined as the ratio between the chip rate and the symbol rate is L.

The data $b_n \in C_M$ is M-PSK modulated at rate $1/T_s$, where T_s is the symbol duration and

$$C_M = \{\ldots, e^{\frac{j2\pi k}{M}}, \ldots\},\ k \in \{0, \ldots, M-1\}. \quad (1)$$

The received signal vector from the antenna array is decorrelated with the spreading code and sampled at the chip rate, resulting in the post-correlation data matrix $\mathbf{Z}_n$ [1]:

$$\begin{aligned} \mathbf{Z}_n = \mathbf{H}_n s_n + \mathbf{N}_n &= \mathbf{G}_n \Upsilon_n \mathbf{D}_n^T s_n + \mathbf{N}_n \\ &= \mathbf{J}_n \mathbf{D}_n^T s_n + \mathbf{N}_n \end{aligned} \quad (2)$$

where $s_n = b_n \psi_n$ is the signal component and ψ_n^2 is the total received power. $\mathbf{H}_n$ is $M \times L$ spatio-temporal propagation channel matrix normalized to $\sqrt{M}$. $\mathbf{D}_n = [D_1, ..., D_p]$ is the time response matrix, where $D_p = [\rho_c(-\tau_p), \rho_c(T_c - \tau_p), \ldots, \rho_c((L-1)T_c - \tau_p)]^T$ is the time-delay impulse response of path p sampled at $1/T_c$, where T_c is the symbol duration. $\mathbf{J}_n$ is the spatio response matrix and corresponds to the propagation matrix $\mathbf{G}_n$ multiplied by the diagonal matrix of power partition over multipaths Υ_n [1]. Finally, $\mathbf{N}_n$ is the noise matrix.

The matrices $\mathbf{Z}_n$, $\mathbf{H}_n$ and $\mathbf{N}_n$ are transformed into (ML)-dimensional vectors by concatenating their columns:

$$\underline{Z}_n = \underline{H}_n s_n + \underline{N}_n \quad (3)$$

where $\underline{Z}_n$, $\underline{H}_n$ and $\underline{N}_n$ denote the resulting vectors.

2.2. Overview of STAR

At each iteration n we assume that we have an estimate of $\underline{H}_n$, $\tilde{\underline{H}}_n$. From this estimate we extract the signal component s_n by spatio-temporal MRC:

$$\tilde{s}_n = \frac{\tilde{\underline{H}}_n^H \underline{Z}_n}{M} \quad (4)$$

then feed this result back in a decision feedback (DFI) scheme to update the channel estimate:

$$\tilde{\underline{H}}_{n+1} = \tilde{\underline{H}}_n + \mu(\underline{Z}_n - \tilde{\underline{H}}_n \hat{s}_n)\hat{s}_n^* \quad (5)$$

where μ is an adaptation step-size, and the feedback signal $\hat{s}_n$ is a reconstructed estimate of the signal component s_n after hard decision over $\tilde{s}_n$, i.e.,

$$\hat{s}_n = \hat{\psi}_n \arg \min_{c_k \in C_M} \|\tilde{s}_n - c_k\|^2. \quad (6)$$

This equation applies a blind DFI procedure to estimate the channel within a constellation invariant phase ambiguity [8]. But, it uses the pilot symbols to estimate and resolve this phase ambiguity [9]. Without pilot symbols the resulting blind version of STAR requires differential decoding of modulated data to remove the phase ambiguity.

3. JOINT TIME-DELAY AND FREQUENCY SYNCHRONIZATION

The joint operation of time-delay estimation and frequency synchronization is accomplished in two steps. First, it estimates the number of multipaths $\hat{P}$, their time delays, their relative power and their magnitude. Then, it determines the carrier-frequency offset. Based on this information an estimate of the spatio-temporal channel is made, and the process is iterated. Key to the present algorithm is the space/time separation procedure that enables us to decouple time and carrier frequency synchronization. The space/time separation has been used in [1] to reduce the identification errors.

From the space/time separation (STS) the spatio-temporal channel $\mathbf{H}_n$ can be reconstructed $\hat{\mathbf{H}}_n = \hat{\mathbf{J}}_n \hat{\mathbf{D}}_n^T$ (instead of $\tilde{\mathbf{H}}_n$) based on estimations of $\hat{\mathbf{D}}_n$ and $\hat{\mathbf{J}}_n$. The column vectors of $\mathbf{J}_n$ can be seen as signal vectors of P sources that differ from one space to another. All these sources propagate in M different spaces but along the same trajectories defined by the matrix $\mathbf{D}_n$, where each multipath time delay correspond to DOA's of sources.

According to this analysis, the variation of multipath time-delays affects only the matrix $\mathbf{D}_n$ and the carrier frequency offset involves the phase of each (m,p)-coefficient of $\mathbf{J}_n$. A joint time and frequency synchronization procedure is then promising.

3.1. Time-Delay and Frequency Acquisition

Based on the STS approach we propose the following algorithm for joint time and carrier frequency acquisition.

1. Initial multipath detection:

   From the spatio-temporal channel estimate $\tilde{\mathbf{H}}_n$ we define a localization spectrum over the possible multipath delays; and limit localization to a simple search over integer multiples of the chip rate (see [3] for more details) to estimate the number of paths $\hat{P}$ and their time-delays. This step allows the estimation of $\hat{\mathbf{D}}_n^T$.

2. Separation of the spatial response matrix $\hat{\mathbf{J}}_n$:

   Once $\hat{\mathbf{D}}_n^T$ is estimated, we use multi-source beamforming to isolate $\hat{\mathbf{J}}_n$ [1]:

   $$\hat{\mathbf{J}}_n^T = (\hat{\mathbf{D}}_n^T \hat{\mathbf{D}}_n)^{-1} \hat{\mathbf{D}}_n^T \tilde{\mathbf{H}}_n^T. \quad (7)$$

   The matrice $\hat{\mathbf{J}}_n$ is then transformed into an (MP)-dimensional vector $\underline{\hat{J}}_n$ by concatenating its columns. We identify its i-th coefficient $\underline{\hat{J}}_{i,n} = \hat{r}_{i,n} e^{j\hat{\phi}_{i,n}}$ by its magnitude $\hat{r}_{i,n}$ and its phase $\hat{\phi}_{i,n}$.

3. Carrier frequency acquisition:

   We consider a slowly varying channel, which means that channel parameters are unchanged over periods

of K symbols while a fixed phase shift (due to carrier offset) is produced between two samples. We buffer the phases of each i-coefficient of $\hat{\underline{J}}_n$ over K symbols and apply a LR-based procedure [2] to estimate Δf. For each diversity finger for $i = 1, \ldots, MP$, we form the following vector:

$$\hat{\Phi}_{i,nK} = [\hat{\phi}_{i,(n-1)K+1}, \cdots, \hat{\phi}_{i,nK}], \quad (8)$$

then estimate Δf at the symbol iteration nK as the slope of a linear regression as follows:

$$\hat{\Delta} f_{i,nK} = \frac{\|R_0\|^2 (R_1^T \hat{\Phi}_{i,nK}) - (R_1^T R_0)(R_0^T \hat{\Phi}_{i,nK})}{2\pi T\{\|R_0\|^2 \|R_1\|^2 - (R_1^T R_0)^2\}}, \quad (9)$$

where $R_0 = [1, \ldots, 1]$ and $R_1 = [1, \ldots, k, \ldots, K]$. Thus, there are MP estimates of the frequency offset. We exploit space-time diversity and minimize estimation errors, by weighted summation over these MP estimates:

$$\begin{aligned} \hat{\Delta} f_{nK} &= \frac{\sum_{i=1}^{MP} \hat{r}^2_{i,(n-1)K+k} \hat{\Delta} f_{i,nK}}{\sum_{i=1}^{MP} \hat{r}^2_{i,(n-1)K+k}} \\ &= \frac{1}{M} \sum_{i=1}^{MP} \left(\frac{\sum_{k=1}^{K} \hat{r}^2_{i,(n-1)K+k}}{K}\right) \hat{\Delta} f_{i,nK}. \end{aligned} \quad (10)$$

For simplicity, we skip the index nK in Δf_{nK} in the following step.

4. Reconstruction of the spatio-temporal channel:

   We reconstruct the spatio-temporal propagation vector $\hat{\mathbf{H}}_n$ by:

$$\hat{\mathbf{H}}_n = e^{-j2\pi \hat{\Delta} f nT} \hat{\mathbf{J}}_n \hat{\mathbf{D}}_n^T. \quad (11)$$

We thereby implement a frequency offset acquisition step in a closed loop structure, where we feed back the estimate of the frequency offset to the input of the receiver:

$$\underline{Z}_n = e^{-j2\pi \hat{\Delta} f nT} (\underline{H}_n s_n + \underline{N}_n). \quad (12)$$

3.2. Time-Delay and Frequency Tracking

After acquisition the DFI procedure of equation (5) is replaced by:

$$\underline{\tilde{H}}_{n+1} = \underline{\hat{H}}_n + \mu(\underline{Z}_n - \underline{\hat{H}}_n \hat{s}_n)\hat{s}_n^* \quad (13)$$

and the extraction of the data signal component in equation (4) is replaced by:

$$\tilde{s}_n = \frac{\hat{H}_n^H \underline{Z}_n}{M}. \quad (14)$$

Reconstraction of an enhanced estimate $\underline{\tilde{H}}_{n+1}$ from $\underline{\tilde{H}}_n$ is implemented by the following joint time delay and frequency tracking loop.

1. Tracking the multipath delays:

   We update the time response matrix $\hat{\mathbf{D}}_n$ with a subspace-tracking equation:

$$\tilde{\mathbf{D}}_{n+1} = \hat{\mathbf{D}}_n + \frac{\eta}{M}(\hat{\mathbf{H}}_n^T - \hat{\mathbf{D}}_n \hat{\mathbf{J}}_n^T)\hat{\mathbf{J}}_{n+1}^*, \quad (15)$$

   where

$$\hat{\mathbf{J}}_{n+1}^T = (\hat{\mathbf{D}}_n^T \hat{\mathbf{D}}_n)^{-1} \hat{\mathbf{D}}_n^T \tilde{\mathbf{H}}_{n+1}^T. \quad (16)$$

   We estimate the multi-paths delays by linear regression, then we rebuild the time-response matrix $\hat{\mathbf{D}}_{n+1}^T$ [1]. This step allows the reconstruction of the spatio-temporal propagation vector $\hat{\mathbf{H}}_{n+1} = \hat{\mathbf{J}}_{n+1} \hat{\mathbf{D}}_{n+1}^T$.

2. Tracking the frequency offset:

   Similarly to the frequency offset acquisition, we estimate the carrier frequency offset error $\hat{\delta} f_n$ by linear regression over successive blocks of length K using the same equations (9) and (10). We update the frequency-offset estimate in equation (11) and (12) as follows:

$$\hat{\Delta} f_{nK} = \hat{\Delta} f_{(n-1)K} + \hat{\delta} f_{nK}. \quad (17)$$

4. PERFORMANCE ANALYSIS

In this section, we compare and analyze the performance of a previous version of STAR (with time-delay synchronization only) and STAR with joint time-delay and frequency synchronization. The numerical results provided are optimized over the adaptation step-size μ for channel identification in STAR [9].

4.1. Simulation Setup

We consider the uplink of M-PSK DS-CDMA with chip rate of 3.840 Mcps operating at a carrier of 1.9 GHz. The spreading factor is $L = 32$ corresponding to a link of 128 Kbaud. The channel is considered Rayleigh fading with Doppler f_D and frequency offset Δf. We assume frequency selective fading with $P = 3$ propagation paths with the same strength. We consider a delay drift of 0.046 ppm. All the parameters of the channel are varying in time.

The base station has $M = 2$ antennas. We implement closed loop power control operating at 1600 Hz and adjusting the power in steps of ± 0.5 dB. A simulated error rate on the power control bit of 5% is used. Finally, we fix the regression length K to 64.

4.2. Frequency Offset Synchronization Performance

First we consider a slow Doppler of 1 km/h, BPSK modulated data at 128 kb/s (i.e., 64 kb/s with rate 1/2 FEC codec) and a frequency offset $\Delta f = 200$ Hz ($\equiv 0.1$ ppm). Figure 1 shows the performance of the frequency offset acquisition

and tracking algorithm. The solid line indicates the exact value of the frequency offset. The semi-dashed curve shows that the estimated frequency offset converges relatively fast, after about 640 symbols (i.e., 5.33 ms), to the desired value within a mean error less than 30 Hz.

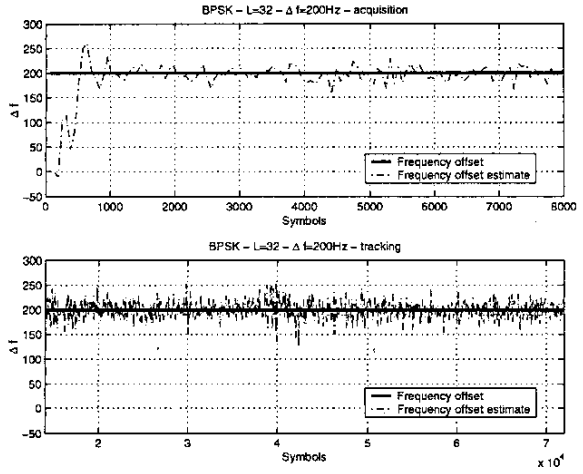

Fig. 1. Acquisition and tracking of constant carrier frequency offset.

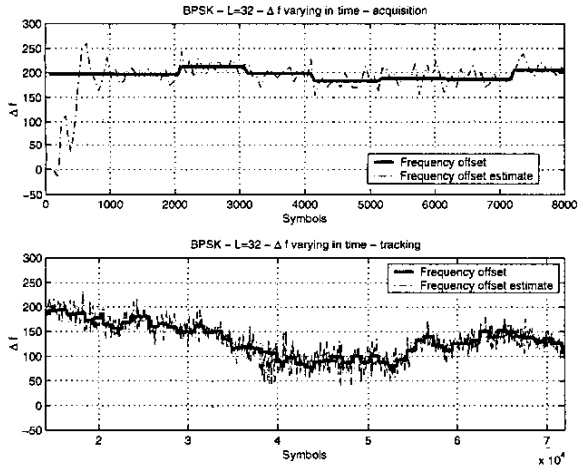

Fig. 2. Acquisition and tracking of time varying carrier frequency offset.

In the previous simulation, we assumed a constant frequency offset. This is a rather simplified assumption. In figure 2, we implement a more realistic time-varying model. We update the frequency offset by adding RV which is a random variable uniformly distributed over $[-\frac{\Delta f}{5}, +\frac{\Delta f}{5}]$; $\Delta f_n = \Delta f_{(n-\alpha)} + RV$. Future work will be based on a more appropriate model obtained from a database of field measurements. Figure 2 shows that the observations related to acquisition and tracking performance holds for both constant and time-varying frequency offset models.

4.3. Impact on Link-level Performance

To illustrate the performance of our algorithm, we plot the link-level curves of STAR with time synchronization assuming perfect frequency recovery (as reference), STAR with time synchronization only, and STAR with joint time and frequency synchronization. 3G standards recommend tight accuracy of 0.1 ppm ($\equiv$ 200 Hz) for the frequency mismatch between the mobile and the base station [10]. Figure 3 shows that even with a frequency offset within the limits of 3GPP, performance degradation is severe. The results of our procedure are identical to those of STAR with perfect frequency recovery, the link-level gain is more than 3 dB for $BER = 5\%$ (before FEC decoding).

To test the recovery capacity of our algorithm we simulated a higher frequency offset of 1 ppm (2 kHz). The link-level gain in figure 4 is more than 10 dB. In both cases of low and high frequency offsets, we note that STAR with joint time-delay and frequency offset synchronization compensates almost completely the performance loss.

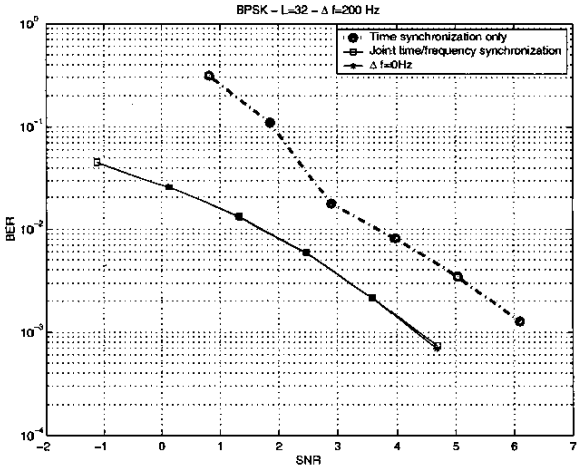

Fig. 3. BER vs. SNR in dB for STAR with time-delay synchronization and STAR with joint time and frequency synchronization for frequency offset = 200 Hz.

In figure 5 the received signal is assumed to be QPSK (256 kb/s), and the frequency offset Δf is 200 Hz. Figure 5 shows that the performance gain for an SER of 5% (before FEC decoding) is almost 1 dB for QPSK. Comparing the results of figures 3 and 5 we notice that the performance gain is higher for BPSK. Indeed, the carrier frequency offset of 200 Hz is the dominant factor in performance loss and QPSK requires a higher SNR to provide the same quality of service of $SER = 5\%$.

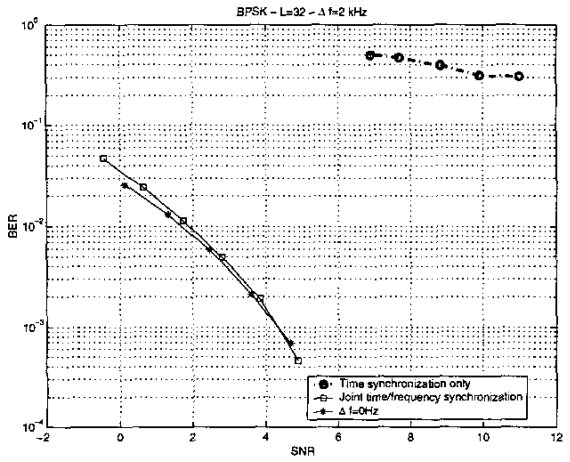

Fig. 4. BER vs. SNR in dB for STAR with time-delay synchronization and STAR with joint time and frequency synchronization for frequency offset = 2 kHz.

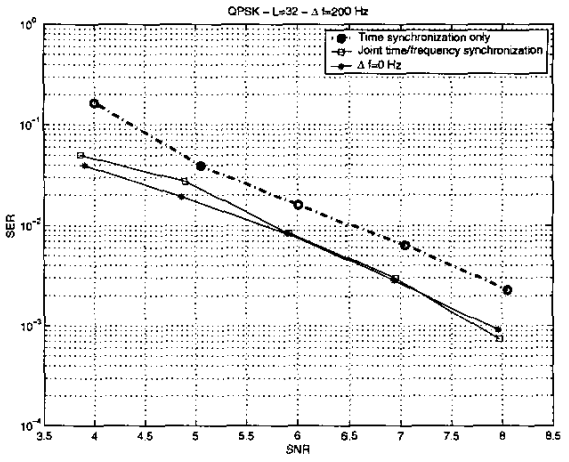

Fig. 5. SER vs. SNR in dB for STAR with time-delay synchronization and STAR with joint time and frequency synchronization for QPSK modulation.

5. CONCLUSIONS

In this contribution we proposed a joint time-delay and frequency synchronization procedure based on the space/time separation that enables us to decouple time and frequency synchronization. This new procedure implements simple Linear Regression (LR) for both frequency and time-delay synchronization. Its incorporation into STAR compensates almost completely the performance loss due to high and low frequency offsets. The link-level gain is more than 3 dB for BPSK (128 kb/s) with a frequency offset of 0.1 ppm. We also find that the performance gains become increasingly important at high frequency offset, where carrier frequency offset recovery is indispensable, and small-constellation modulation, where SNR is lower.

6. REFERENCES

[1] S. Affes, P. Mermelstein, "A new receiver structure for asynchronous CDMA: STAR-the spatio-temporal array-receiver", *IEEE J. Select. Areas in Comm.*, vol. 16, no. 8, pp. 1411-1422, October 1998.

[2] S. Affes, J. Zhang, and P. Mermelstein, "Carrier frequency offset recovery for CDMA array-receivers in selective Rayleigh-fading channels", *proc. of 55th IEEE VTC'2002*, Vol. 1, pp. 180-184. Birmingham, USA.

[3] K. Cheikhrouhou, S. Affes, and P. Mermelstein, "Impact of synchronization on performance of enhanced array-receivers in wideband CDMA networks", *IEEE J. Select. Areas in Comm.*, vol. 19, no 12, pp. 2462-2476, December 2001.

[4] L. Tong, "Joint blind signal detection and carrier recovery over fading channel", *proc. Of IEEE ICASSP*, May 1995, pp. 1205-1208.

[5] H. A. Cirpan and M. K. Tsatsanis, "Maximum likelihood blind channel estimation in the presence of frequency shifts", *Proc. 30th Asilomar Conf. Signals, Systems, and Computer*, Pacific Grove, CA, Nov. 1996.

[6] M. Eric and M. Obradovic, "Subspace-based joint time-delay and frequency-shift estimation in asynchronous DS-CDMA systems", *Electron. Lett.*, vol. 33, pp. 1193-1195, July 1997.

[7] K. Li and H. Liu, "An analytic solution to joint channel and carrier offset estimation in CDMA", *IEEE Signal Processing Lett.*, vol 5, pp. 234-236, Sep. 1998.

[8] S. Affes and P. Mermelstein, "Adaptive Space-Time Processing for Wireless CDMA", *Book Chapter, Adaptive Signal Processing: Application to Real-World Problems*, J. Benesty and A.H. Huang, Eds., Springer, Berlin, to appear, January 2003.

[9] S. Affes, N. Kandil, and P. Mermelstein, "Efficient Use of Pilot Signals in Wideband CDMA Array-Receivers", *Proc. of IEEE ICC'03*, Anchorage, Alaska, USA, to appear, May 11-15, 2003.

[10] 3GPP TS 25.101 V5.4.0, 3rd Generation Partnership Project (3GPP), Technical Specification Group (TSG), Radio Access Network (RAN), UE Radio Transmission and Reception (FDD), September 2002.